



expression for these turbulence stresses can be found with definite physical meanings, some universal modelings with fixed constant coefficients would be possible. The trouble is that the concrete content of these turbulence stresses is never known. Therefore, modelings with incorrect stresses terms have to struggle with coefficient adjustment. The concept of zonal modeling, suggested by Kline (1981) at the 1980/1981 Standord Conference on Computation of Complex Turbulent Flows, implies that there is no universal turbulence modeling and the coefficients may depend on the flow type, which in turn implies that a user has to choose the qualitative flow type and its corresponding coefficients. By definition, however, a modeling should have coefficients which will be applied without case-to-case adjustment by the user. Otherwise the modeling loses its generality and creditability.

Despite many modelers are strongly biased towards Reynolds-stress modeling, stress-transport modelings have not lived up to their promise. It seems that along the first approach, the road is endless so long as the problem of nonlinearity is imminent.

#### THEORETICAL DEVELOPMENT

In the last decade, chaos and fractal have become the frontiers of research in non-linear dynamics. It has been learned that the seemingly chaotic events resulting from the orderly physical laws, are not truly formless chaos, but exhibit underlying coherent patterns and possess fractal structures. This modern interpretation of chaos has been gradually replacing the conventional view that the order emerges from the underlying formless chaos. Along with the discovery of chaotic phenomena in all areas of nonlinear dynamics, it is also recognized that nonlinear difference and differential equations can admit bounded, nonperiodic solutions which exhibit randomized behavior even though no random parameters appear in the original governing equations (e.g. Moon, 1987) Turbulence is one of the few remaining unsolved problems in classical physics. The recent discovery of deterministic systems exhibiting chaotic oscillations has created much optimism about understanding the mysteries of turbulence. Recent studies on fractals have been focused on fractal geometry dimension and attractors (e.g. Orbach, 1986 and Moon, 1987). So far as the fractal dynamics is concerned, it has not reached its pragmatic stage of analyzing the dynamic process of a fractal system.

Since a turbulent field is governed by a giant system of multiple strange attractors, the concept and the method of attractors seem far away to give an accountable description of turbulence. It is necessary to try to find some other alternatives within the concept of fractals. It is indeed the intention of the present effort to introduce a general analytical-averaging method for nonlinear equations, developed within the fractal concept. Application of this technique to turbulence opens a new way for turbulence modeling, indicating the fruitfulness of the above mentioned second approach.

#### A GENERAL FRACTAL ANALYTICAL METHOD FOR NONLINEAR EQUATIONS

In dealing with the generalities of all disordered systems, fractal claims that random recurrent behavior gives rise to a family of remarkably similar patterns, which appear on different scales at the same time with abrupt boundary and sudden transitions. Despite the fact that accumulation of recurrent patterns gives apparent chaos, the quasi-self-similar patterns imply that the recurrent behavior must be governed by the same nonlinear equation, but with different scales at the same time.

Fractal has unforeseen importance on the nonlinear science. It points out that the spatio-temporal dimension is not an integer, but a fraction, and there is hidden orderliness behind the apparent disorder phenomena. The change of outlook on space and time would have dramatic impact both in the Natural science and the Philosophy. On the side of the nonlinear science, it lays a physical foundation of analytical-averaging method for the nonlinear equation. After several bifurcations, an unstable nonlinear equation usually produces chaotic solutions. Among numerous chaotic solutions, only their average behavior is meaningful and controllable. But the control equation describing an averaged chaotic phenomenon differs from its original nonlinear equation. Only after necessary mathematical treatment can the average control equation be obtained. Ordering or quasi-ordering is determined by the original nonlinear equation. Accumulation of recurrent patterns with different scales presents apparently disordered chaotic patterns. Based on this concept, a general analytical method seeking for the control equation of chaos is suggested as follows:

1. From the D'Alembert's principle, any nonlinear equation may be considered as a generalized dynamically balanced system. Upon multiplying the original nonlinear equation by a small scaled displacement of perturbation, it yields the corresponding terms of perturbation work controlled by the equation within the small scaled space.
2. Through the virtual work analysis on the perturbation work, distinguish the active and passive work terms; the active terms being responsible for the perturbation work production the passive ones for the work redistribution.
3. A new equation is obtained by adding the corresponding active perturbation force terms to the original equation. This new equation is able to describe the average behavior of the chaotic system with a second order of accuracy.
4. Repeat the procedures 1-3 with even smaller scales to obtain a new equation with a higher order of accuracy.

Nonlinear functions do not have additivity. But after discarding the passive terms, the active generalized perturbation forces are addible. In the meantime, when the active terms are added to the original equation, all dependent variable of the new equation became averaged quantities and an average equation has been obtained.

THE PERTURBATION EQUATION OF THE NAVIER-STOKES EQUATION

Turbulence is a typical fractal phenomenon. The Navier-Stokes equation is usually applied to the total time varying velocity field. For a laminar flow with a single scale, the Navier-Stokes equation gives a single determinate solution. For a turbulent flow with multiple scales, it gives chaotic solution. Chaotic flow field usually has infinite layers of scales. Therefore, the Navier-Stokes equation can give accurate solutions for turbulent flows only when the smallest scale valid under the concept of continuum, is adopted. When discrete mathematical method is used to solve the Navier-Stokes equation, any of its determinate solution is only a mathematically expected distribution upon which there must always be added some stochastic fluctuations with scales less than the adopted size of grid. In other words, there always exists an accompanying noise or perturbation field along with the solution of the Navier-Stokes equation. In the sense of fractal, there must always be some self-similar subpatterns with even smaller scales within the flow simulating and confirming the flow patterns of reality. This is the reason why turbulence models must be performed instead of employing the Navier-Stokes equation for practical engineering calculations. Nevertheless, the Navier-Stokes equation is still the starting point for the analysis of turbulence. The aim of the analysis is to find out the precise expression of the effect of the perturbation field on the average equation of turbulence, i.e. the alternative expression of Reynolds stress terms.

Let

$$\hat{V} = \hat{V}_E + \hat{V}', P = P_E + P' \quad (1)$$

where  $\hat{V}_E, P_E$  are mathematically expected values of the velocity and the pressure,  $\hat{V}', P'$  are their perturbation values and  $\hat{V}, P$  are their real values. Both the real and the expected values satisfy the Navier-Stokes equation. They belong to the infinitely numerous chaotic solutions of the nonlinear equation. In fact, both  $\hat{V}$  and  $\hat{V}_E$  correspond to two distinct realizations of the fractal dynamical system, each obeying the Navier-Stokes equation. From the Navier-Stokes equation, one obtains

$$\frac{D\hat{V}_E}{Dt} = -\frac{\nabla P_E}{\rho} + \nu \nabla^2 \hat{V}_E \quad (2)$$

$$\frac{D\hat{V}}{Dt} = \frac{D(\hat{V}_E + \hat{V}')}{Dt} = -\frac{1}{\rho} \nabla (P_E + P') + \nu \nabla^2 (\hat{V}_E + \hat{V}') \quad (3)$$

Subtracting Eq. (2) from (3) yields

$$\begin{aligned} \frac{\partial \hat{V}'}{\partial t} + (\hat{V}_E \cdot \nabla) \hat{V}' + (\hat{V}' \cdot \nabla) \hat{V}_E \\ + (\hat{V}' \cdot \nabla) \hat{V}' = -\frac{1}{\rho} \nabla P' + \nu \nabla^2 \hat{V}' \end{aligned} \quad (4)$$

Equation (4) and the Poisson equation of the fluctuating pressure given by

$$-\frac{1}{\rho} \nabla^2 P' = \nabla \cdot [(\hat{V}_E \cdot \nabla) \hat{V}' + (\hat{V}' \cdot \nabla) \hat{V}_E + (\hat{V}' \cdot \nabla) \hat{V}']$$

yield

$$\frac{\partial \hat{V}'}{\partial t} - \nu \nabla^2 \hat{V}' = C \quad (5)$$

where C is the constant of integration determined by the boundary conditions of the fluctuating velocity and pressure. Equation (4) may be expressed as

$$\begin{aligned} C + \nu \nabla^2 \hat{V}' + (\hat{V}_E \cdot \nabla) \hat{V}' + (\hat{V}' \cdot \nabla) \hat{V}_E \\ + (\hat{V}' \cdot \nabla) \hat{V}' = -\frac{1}{\rho} \nabla P' + \nu \nabla^2 \hat{V}' \end{aligned} \quad (6)$$

Equation (2) with its boundary condition may have a determinate solution for a group of streamlines. From the viewpoint of analytical mechanics, the equation and its boundary conditions are still a set of incomplete constraints for the chaotic state. Upon taking the natural frame of the streamline group as the generalized coordinates, the perturbation force may be interpreted as the generalized force acting within the generalized system of coordinates. Therefore, through the virtual work analysis, and subsequently adding these perturbation forces to Eq. (2) may directly give the perturbation equation of the Navier-Stokes equation.

According to the rate of deformation tensor given by

$$\frac{\partial u_j}{\partial x_j} = \overset{\rightharpoonup}{S} + 1/2 (\nabla \times \hat{V}) \quad (7)$$

where  $\overset{\rightharpoonup}{S}$  is the rate of strain tensor, and  $1/2 (\nabla \times \hat{V})$  is the rotation tensor. One may use a method analogous to the Prandtl's mixing length concept

( $v' = l \frac{\partial u}{\partial y}$ ) to obtain

$$\hat{V}' = \frac{\partial u_j}{\partial x_j} \delta \hat{r} = \overset{\rightharpoonup}{S} \cdot \delta \hat{r} + 1/2 (\nabla \times \hat{V}) \times \delta \hat{r}$$

or

$$\hat{V}' = \nabla\phi + 1/2 (\nabla \times \hat{V}) \times \delta\hat{r} \quad (8)$$

where  $\delta\hat{r}$  is a perturbation displacement and  $\nabla\phi$  is the velocity of strain. Due to the local discrete character of turbulence (the particle character of

turbulent eddies),  $\delta\hat{r}$  may be considered as a local spatio-temporal constant vector much larger than the differential scales. This assumption introduces discreteness into the treatment of tur-

bulence. Upon multiplying Eq. (6) by  $\delta\hat{r}$  and substituting Eq. (8) into it, one may obtain the virtual work as

$$\begin{aligned} \delta E &= \hat{F}_g \cdot \delta\hat{r} = \delta\hat{r} \cdot \left[ -\frac{1}{\rho} \nabla p' + v \nabla^2 \hat{V} \right] \\ &= \delta\hat{r} \cdot \left[ c + v \nabla^2 (\nabla\phi) + (\hat{V}_E \cdot \nabla) \nabla\phi + (\nabla\phi \cdot \nabla) \nabla\phi \right. \\ &\quad \left. + 1/2 (\nabla \times \delta\hat{r} \cdot \nabla) \nabla\phi - \frac{v}{2} (\delta\hat{r} \cdot \nabla) \nabla \times \hat{\Omega} \right] \quad (9) \end{aligned}$$

where  $\hat{F}_g$  represents the generalized perturbation force. After discarding the passive terms, the generalized perturbation force is addible to the right side of Eq. (2) and then let the velocity variables have new values to obtain a new equation, which includes the interaction between the two distinct fractal flows of different scales and

describes their average behavior. Upon adding  $\hat{F}_g$  to the right side of Eq. (2) and treating all parameters as the ensemble average, one obtains the perturbation equation of the Navier-Stokes equation as:

$$\begin{aligned} \frac{D\tilde{V}}{Dt} &= -\frac{1}{\rho} \nabla p + v \nabla^2 \tilde{V} + (\tilde{V} \cdot \nabla) \nabla\phi + \frac{1}{2} (\nabla \times \delta\tilde{r} \cdot \nabla) \nabla\phi \\ &\quad + (\nabla\phi \cdot \nabla) \nabla\phi + v \nabla^2 (\nabla\phi) - \frac{v}{2} (\delta\tilde{r} \cdot \nabla) \nabla \times \tilde{\Omega} + c \quad (10) \end{aligned}$$

where the tildes, "~", denotes the mean values. The indefinite integral constant  $c$  has no influence on the discrete numerical calculation of turbulent flows. It is thus negligible in the differential treatment of turbulence.

Obviously, Eq. (10) is an alternative to the Reynolds equation, and provides a concrete expression of turbulent stress terms. The physical interpretation of the extra turbulence stresses has been precisely described by the five extra terms on the right side of Eq. (10). In fact, the equation is the physical equation of turbulence with a second order accuracy, which has been sought after for a long time. A detailed discussion on this equation has been reported elsewhere (Gao, 1989a).

## THE ESSENCE OF EXTRA NONISOTROPIC STRESSES

Shearing is the most obvious reason of production of turbulent kinetic energy. However, the curvature of streamline, the stretching or compression of streamline and the interaction between the large and small turbulent eddies may also play important roles in producing turbulent stresses. All non-shearing stresses are named extra stresses. They must be appropriately considered for complex turbulent flows. The momentum equation based on the concept of eddy viscosity is

$$\frac{D\hat{V}}{Dt} = -\frac{1}{\rho} \nabla p + (v_L + v_T) \nabla^2 \hat{V} \quad (11)$$

This equation is a result of analogous simulation of turbulent eddy viscosity to molecular viscosity. A rigorous derivation of the equation is lacking.

To simplify the perturbation Eq. (10), one assumes that the perturbation velocity  $\nabla\phi$  and the

perturbation displacement  $\delta\tilde{r}$  are locally constant and contribute as part of the eddy viscosity,  $v_T = c' \nabla\phi \delta\tilde{r}$ , where  $c'$  is an empirical coefficient. Equation (10) now becomes

$$\begin{aligned} \frac{D\tilde{V}}{Dt} &= -\frac{1}{\rho} \nabla p + (v_L + v_T) \nabla^2 \tilde{V} + \frac{1}{2} (\nabla \times \delta\tilde{r} \cdot \nabla) \nabla\phi \\ &\quad + (\tilde{V} \cdot \nabla) \nabla\phi - \frac{v_L}{2} (\delta\tilde{r} \cdot \nabla) (\nabla \times \tilde{\Omega}) \quad (12) \end{aligned}$$

with  $v_T \nabla^2 \tilde{V} = (\nabla\phi \cdot \nabla) \tilde{V} + v \nabla^2 (\nabla\phi)$

$v \nabla^2 (\nabla\phi)$ , representing the effect of positive dispersion on the turbulent stresses which is one of the most important features of turbulence (Karweit, 1985), has been absorbed into the viscosity coefficient, and

$$(\nabla\phi \cdot \nabla) \nabla\phi = \nabla\phi \delta\tilde{r} \nabla^2 \tilde{V}$$

Comparing Eq. (12) with Eq. (11), one recognizes that there are three extra turbulent stresses in Eq. (12): the vorticity term in which the effect of streamline curvature is included; the convective term of perturbation velocity in which the effect of streamline stretching or compression is included; and the last term consisting of the perturbation displacement and the secondary derivative of the vorticity, which reflects the effect of interaction between large and small eddies. If a correct modeling of these extra terms can be accomplished, problems with these extra nonisotropic stresses can be properly dealt with. These three extra terms also reveal the physical essence of these extra stresses, which are the direct

results of the convective perturbation velocity and the interaction between vorticity and perturbation parameters. They also simultaneously show the convective transportation (expressed by the two preceding terms) and the discrete character (expressed by the last term) of turbulence.

A brief observation of Eq. (12) may also reveal the shortcomings of the prevailing turbulence modelings. For instance, in the eddy-viscosity models, only  $v_T \nabla^2 \tilde{v}$  is considered; in the large eddy simulation, only  $v \nabla^2 (\nabla \phi)$  is considered; in the Reynolds stress modeling, the discreteness term,

$$-\frac{v}{2} (\delta \tilde{r} \cdot \nabla) \nabla x \tilde{\Omega},$$

has not been considered.

Anisotropy, as a direct result of nonlinearity, is a basic characteristic of turbulent flows, and is not the property of the fluid. Adopting the Boussinesq's eddy-viscosity concept, a traditional treatment for anisotropy is to look for an anisotropic viscosity coefficient. But from the viewpoint of random movement, it is known that the local isotropy of turbulent eddies prevails. The movement of eddies has a strong tendency to isotropy due to the isotropic stochastic collision, except for those occasions where the extra stresses cause eddies moving in a particular direction. Therefore, in a general sense, adoption of an isotropic turbulent viscosity coefficient  $\mu_T$  at any point of the flow field is more convincing. The assumption of isotropic  $\mu_T$  is in consistence with stochastic property of turbulence. Anisotropy should be expressed by the extra stresses in the momentum equation. From Eq. (10), the corresponding turbulence stress tensor can be interpreted as

$$\begin{aligned} \tau_{ij} = & \tilde{v} \nabla \phi + \frac{1}{2} (\tilde{\Omega} x \delta \tilde{r}) \nabla \phi + \nabla \phi \nabla \phi + v \nabla (\nabla \phi) \\ & - \frac{v}{2} \delta \tilde{r} (\nabla x \tilde{\Omega}) \end{aligned} \quad (13)$$

It is obvious that with the effects of the ordinary and the extra stresses, Eq. (13) will display non-isotropic features.

#### TURBULENCE MODELING

The perturbation equation of the Navier-Stokes Eq. (10) contains two turbulent parameters: the perturbation velocity  $\nabla \phi$  and the perturbation displacement  $\delta \tilde{r}$ .

If both of them can be correctly described by differential equations, complex turbulent flow problems can be dealt with completely within the realm of the two-equation modeling. There exist many ways to modeling the Eq. (10). As a simulation of molecular motion, turbulent viscosity usually consists of a length scale, a velocity scale and an experimentally determined

coefficient, i.e.  $v_T = c \tilde{v}$ . In order to model the perturbation equation, the velocity of strain  $\nabla \phi$  may be chosen as the velocity scale and the perturbation displacement  $\delta \tilde{r}$  may be chosen as the length

scale. Changing the positions of  $\nabla \phi$  and  $\delta \tilde{r}$  to bring them together to form the turbulent viscosity  $v_T$ , one may effectively consider that they are locally constants and neglect their spatial differentials. One of these attempts of modeling is given by Gao (1989b). In this scheme a set of new control equations for incompressible turbulent flow, i.e., continuity, momentum, turbulent kinetic energy, its dissipation and the energy equations, are formulated as:

scale. Changing the positions of  $\nabla \phi$  and  $\delta \tilde{r}$  to bring them together to form the turbulent viscosity  $v_T$ , one may effectively consider that they are locally constants and neglect their spatial differentials. One of these attempts of modeling is given by Gao (1989b). In this scheme a set of new control equations for incompressible turbulent flow, i.e., continuity, momentum, turbulent kinetic energy, its dissipation and the energy equations, are formulated as:

$$\frac{\partial u_i}{\partial x_i} = 0 \quad (14)$$

$$\begin{aligned} \frac{\partial u_i}{\partial t} + u_j \frac{\partial u_i}{\partial x_j} = & - \frac{1}{\rho} \frac{\partial p}{\partial x_i} + \frac{\partial (v_L + v_T)}{\partial x_j} \left( \frac{\partial u_i}{\partial x_j} + \frac{\partial u_j}{\partial x_i} \right) \\ & + \Omega_{ij} \frac{\partial v_T}{\partial x_j} + C_3 \epsilon_i u_j \frac{\partial \sqrt{k}}{\partial x_j} \\ & - C_0 v_T \frac{k^{3/2}}{\epsilon} \epsilon_i \epsilon_{ijk} \frac{\partial^2 \Omega_k}{\partial x_j \partial x_i} \end{aligned} \quad (15)$$

$$\frac{\partial k}{\partial t} + u_j \frac{\partial k}{\partial x_j} = \frac{1}{\rho} \frac{\partial}{\partial x_j} \left( \frac{\mu_T}{\sigma_k} \frac{\partial k}{\partial x_j} \right) + \frac{G_k}{\rho} - \epsilon \quad (16)$$

$$\begin{aligned} \frac{\partial \epsilon}{\partial t} + u_j \frac{\partial \epsilon}{\partial x_j} = & - \frac{1}{\rho} \frac{\partial}{\partial x_j} \left( \frac{\mu_T}{\sigma_\epsilon} \frac{\partial \epsilon}{\partial x_j} \right) \\ & + C_1 \frac{\epsilon G_\epsilon}{k + (2v_L \epsilon)^{1/2}} - C_2 \frac{\epsilon^2}{k + (2v_L \epsilon)^{1/2}} \end{aligned} \quad (17)$$

$$\frac{\partial h}{\partial t} + u_j \frac{\partial h}{\partial x_j} = \frac{1}{\rho} \frac{\partial p}{\partial t} + \frac{1}{\rho} u_j \frac{\partial p}{\partial x_j} + \frac{1}{\rho} \frac{\partial}{\partial x_j} \left( \lambda \frac{\partial T}{\partial x_j} \right) + \frac{\phi}{\rho} + \frac{\psi}{\rho} \quad (18)$$

$$G_k = \max (I - II - III, 0) \quad , \quad G_\epsilon = \max (I - II, 0)$$

$$\begin{aligned} I = & \mu_T \left[ \left( \frac{\partial u_i}{\partial x_j} + \frac{\partial u_j}{\partial x_i} \right) \frac{\partial u_i}{\partial x_j} + \left( \frac{\partial u_i}{\partial x_j} - \frac{\partial u_j}{\partial x_i} \right) \frac{\partial u_j}{\partial x_i} \right] \\ = & \mu_T \left( \frac{\partial u_i}{\partial x_j} + \frac{\partial u_j}{\partial x_i} \right) \frac{\partial u_i}{\partial x_j} - \frac{1}{2} \mu_T \Omega_{ij}^2 \quad , \end{aligned}$$

$$II = C_3 \epsilon_i u_j \sqrt{k} \frac{\partial u_i}{\partial x_j} \rho,$$

$$III = C_0 \mu_T \frac{k^{3/2}}{\epsilon} \epsilon_l \epsilon_{ijk} \frac{\partial \omega_k}{\partial x_j} \frac{\partial u_i}{\partial x_l},$$

$$\omega_{ij} = \frac{\partial u_j}{\partial x_i} - \frac{\partial u_i}{\partial x_j}, \quad \mu_T = C_\mu \frac{\rho k^2}{\epsilon},$$

$$\text{when } u_i \geq 0, \quad \epsilon_i = \epsilon_j = 1 \\ u_i < 0, \quad \epsilon_i = \epsilon_j = -1$$

For the dissipation function  $\phi$ ,  $\phi = \max (I-II, 0)$

$$+ \mu_L \left( \frac{\partial u_i}{\partial x_j} + \frac{\partial u_j}{\partial x_i} \right) \frac{\partial u_i}{\partial x_j}$$

For the dispersion function  $\psi$ ,  $\psi = - III$ .

Various constants and coefficients related to this modeling are given in Table I.

Table 1. The coefficients for the Rectangular system of coordinates.

$C_0$	$C_1$	$C_2$	$C_3$
$III \geq 0, 0.30$	1.44	1.92	0.16
$III < 0, 0.0$			

$\sigma_k$	$\sigma_\epsilon$	$C_\mu$
1.0	1.3	0.09

As discussed previously (Gao, 1989b) due to the spatio-temporal instability, intermittency of turbulent flow is the basic reason that the principle directions of stress and strain are non-coincident with each other. This is why the Boussinesq's eddy-viscosity model fails. The task of turbulence modeling is to resolve the incompatibility of the constitutive relations of the viscous flow with the non-Newtonian property of the intermittent turbulent flow. In this sense, all the extra stresses, added to the momentum equations as presented in Eq. (10), cannot be interpreted as standard tensors. This present modeling by Gao (1989b), however, is a modification of the original k- $\epsilon$  modeling by Launder and Spalding (1974) by taking advantage of their previous tremendous achievement. In order to bring all the extra terms into tensorial expression, an effort to use the summation subscripts has been applied to them.

Based on the nonlinear fractal analysis, the new modeling has extra terms of stretching, rotation and negative dispersion, which reflect the non-linear coherent property of turbulence. On the other hand, the empirical coefficients reflect the stochastic nature of turbulence. Many perplexing problems of turbulence, such as anisotropy, turbulence energy inversion (Sommeria, 1986), cut-off of the turbulence energy spectra, intermittency and coherent structure may be explained theoretically and simulated numerically by this nonlinear modeling.

### DISCUSSION OF COMPUTED RESULTS

By adopting the procedures suggested by Patankar (1981) numerical computations for many complex turbulent flows have been performed with the improved turbulence modeling. The results of these calculations are respectively discussed in the following:

#### 1. The Anomaly of the Round Jet/Plane Jet

The computed and measured behavior for the plane and the round jets are compared in Figs. 1-3, and in Table 2. The corresponding kinetic energy profile, shown in Figs. 1 and 2, are in satisfactory accord. The difference in the shape of the turbulence kinetic energy profiles between the round and plane jets is correctly reproduced by these numerical computations. The improvement of the k profile of the round jets, especially in the region near the axis, is mainly attributable to the extra stretching term in the momentum equation. In the case of the round jet, the strength of the velocity decay in this region is far greater than that in the plane jet. Since the velocity decay effectively increases the kinetic energy production, the k profile of the round jets exhibits a monotonic decrease from the axis while the k profile of the plane jets exhibits a hump with its maximum at  $y = 0.65 y_{1/2}$ . The most interesting

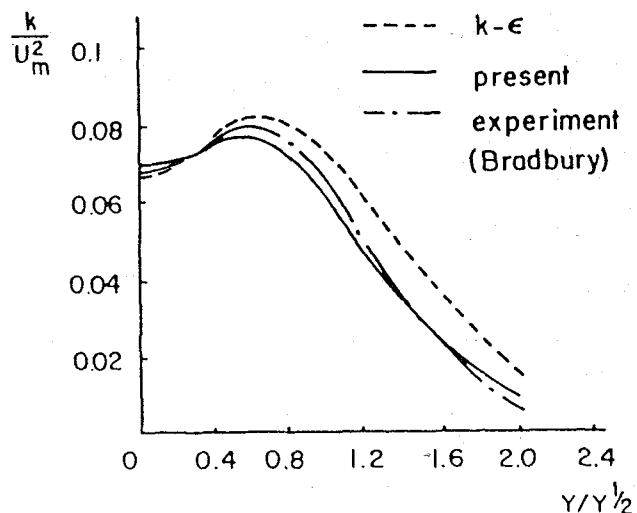


Fig.1. Turbulence Kinetic Energy Profile of a Plane Jet in Stagnant Surrounding

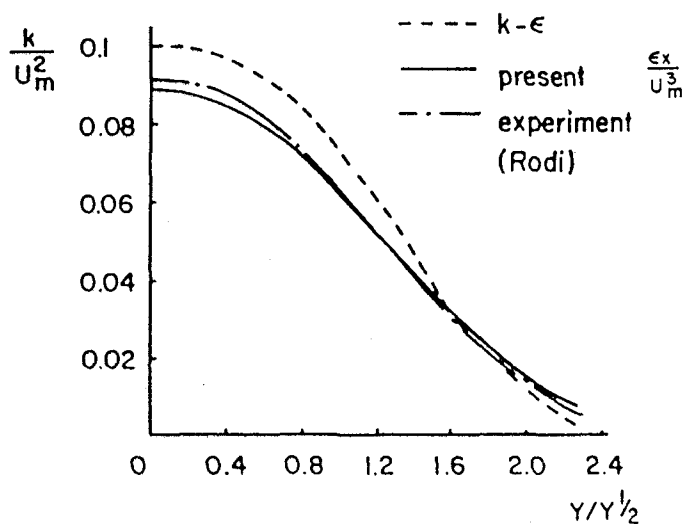


Fig.2. Turbulence Kinetic Energy Profile of a Round Jet in Stagnant Surrounding

results appear in Table II, which lists the rates of spread of the two flows including that of the experimental data. It also includes the results from the Algebraic stress model and the Reynolds stress transport model. Obviously the anomaly of the round jet/plane jet has been adequately resolved (Hanjalic, 1988). The reason for the improvement of the spread rate is traced to the extra stretching term in the momentum equation. The component of the stretching term in the

y-direction is  $C_3 V \frac{\partial \sqrt{k}}{\partial y}$ . From Figures 1 and 2,

it is shown that this term always suppresses the rate of spread for the round jet, while it is positive within the region from the axis to  $y = 0.65y_{1/2}$  for the plane jet, which helps to increase the rate of spread. Shown in Figure 3 are the measured and predicted dissipation profiles of the round jets. Since there is no extra stretching term in the dissipation production  $G_e$  of the present modeling, a hump-like profile of dissipation has been obtained. If this extra stretching term is also included into  $G_e$ , the level of  $\epsilon$  decreases monotonically from the axis, similar to the  $k$  profile in the round jets. This gives an important support to the opinion that  $G_k$  and  $G_e$  should not contain the same element, and the extra stretching term should appear only in  $G_k$ .

Table II Rates of Spread of Plane and Round Jets

Flow	Experiment	Original k- $\epsilon$ Model	ASM	RST	Present Model
Plane jet	0.110	0.108	0.114	0.108	0.111
Round jet	0.086-0.093	0.114	0.149	0.121	0.092

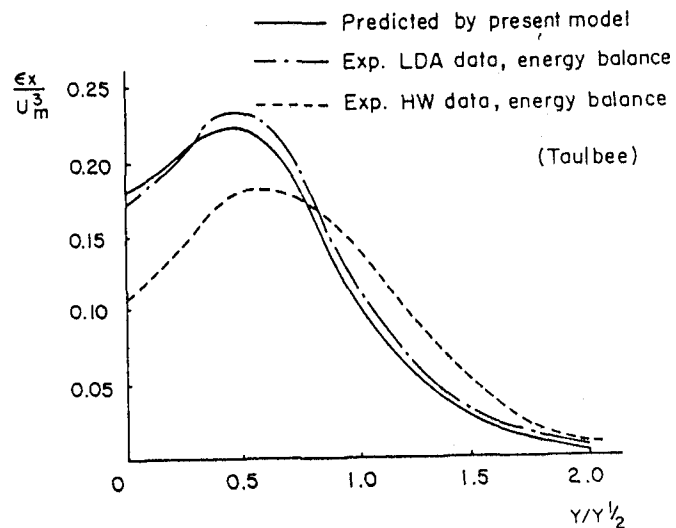


Fig.3. The Measured and the Predicted Profiles of a Round Jet (Dissipation Rate of the Turbulence Kinetic Energy)

## 2. Near Wall Flow

Since the modeled differential equation for free turbulence yields incorrect results near a wall, various ad hoc functions (there are at least five functions of this kind in the  $k-\epsilon$  modeling) are conventionally added in an effort to eliminate this shortcoming. Since the present modified  $k-\epsilon$  method is based upon a thorough consideration of the non-linearity of turbulent flow, the appearance of the proposed modeling undergoes a substantial change. Group I of  $G_k$  always subtracts the term

$\frac{1}{2} \mu_T \Omega_{ij}^2$ , which accounts for a significant improvement of the shortcoming of the original  $k-\epsilon$  modeling. It is well known that the original  $k-\epsilon$  modeling invariably predicts a higher turbulence intensity and turbulent viscosity in the near wall region ( $Y^+ < 40$ ). The cut-off state of  $G_k$  and  $G_e$  in the region of  $Y^+ = 10$  also offers an important contribution to the correct prediction in the near-wall region. An interesting discovery arising from this improvement is the modified  $k-\epsilon$  modeling is effective for both the free flow and the near-wall flow. No additional function is needed in this improved modeling.

### 3. Three-Dimensional Calculation of a Centrifugal Compressor

With this Gao's modeling, Bo and Bosman (1989) at the University of Manchester Institute of Science and Technology, computed a three-dimensional flow field of a centrifugal compressor, and achieved a complete success. The grid of calculated flow field is shown in Fig. 4. The computed results at the section No. 25 by the original k- $\epsilon$  model and the present model are shown in Figs. 5 and 6, respectively. Fig. 7 presents the experimentally measured results in the same section. In comparing these sets of results, it is obvious that the present modeling gives very good prediction of the secondary flow vortices in scale, form, position and the flow direction, very similar to the experimental data. However, for the original k- $\epsilon$  modeling, the vortex on the suction side almost disappears. Both the turning points of the flow direction and the velocity profile of the secondary flow vortices are qualitatively incorrect, and the poor results cannot be corrected despite wide adjustment on its empirical coefficients. It has been found that the extra stretching and rotation terms of the new modeling are responsible for the correct prediction, which exhibits the characteristic of strong stretching and sharp rotation in the centrifugal compressor, (Cumpsty, 1989).

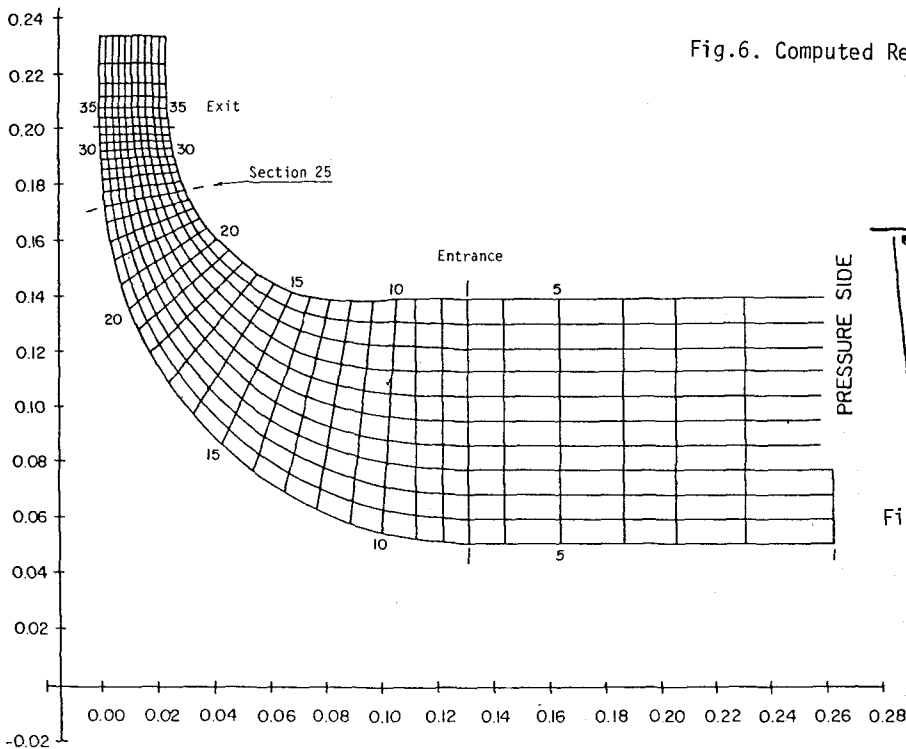


Fig. 4. The Computational Grid for the Eckardt Compressor

### 4. Swirling Flows

Another important improvement was observed in the confined sudden-expansion swirling flows by Xu and Gao (1990). With the new modeling, the form of the recirculating zone, the composite vortex profile of the tangential velocity, the preceding vortex roll behind the recirculating zone, and the

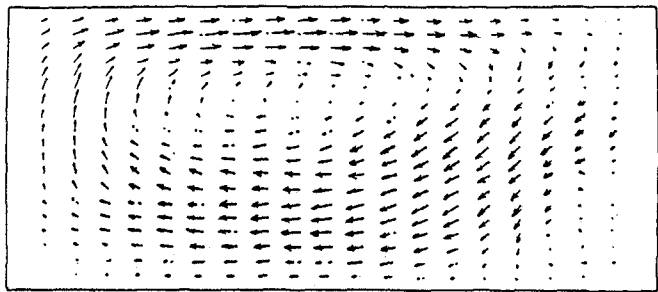


Fig. 5. Computed Results from the Ordinary K-E Model

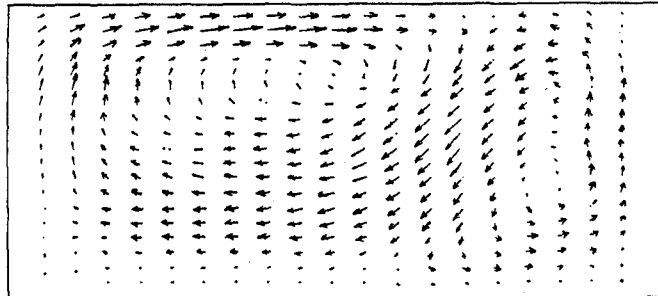


Fig. 6. Computed Results from the Improved Model

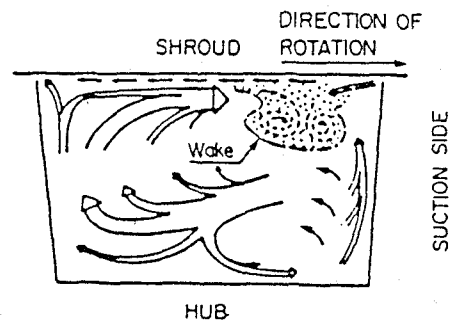


Fig. 7. Experimental Data for the Eckardt Compressor

profile of the axial velocity within the recirculating zone are all correctly reproduced through numerical computations. Fig. 8 shows the comparison of the axial and tangential velocity profiles between the experimental and the numerically predicted results. The original k- $\epsilon$  modeling failed to give the preceding vortex roll (Fig. 8a), the outer composite vortex (Fig. 8b) and the deficit of the axial velocity near the central axis



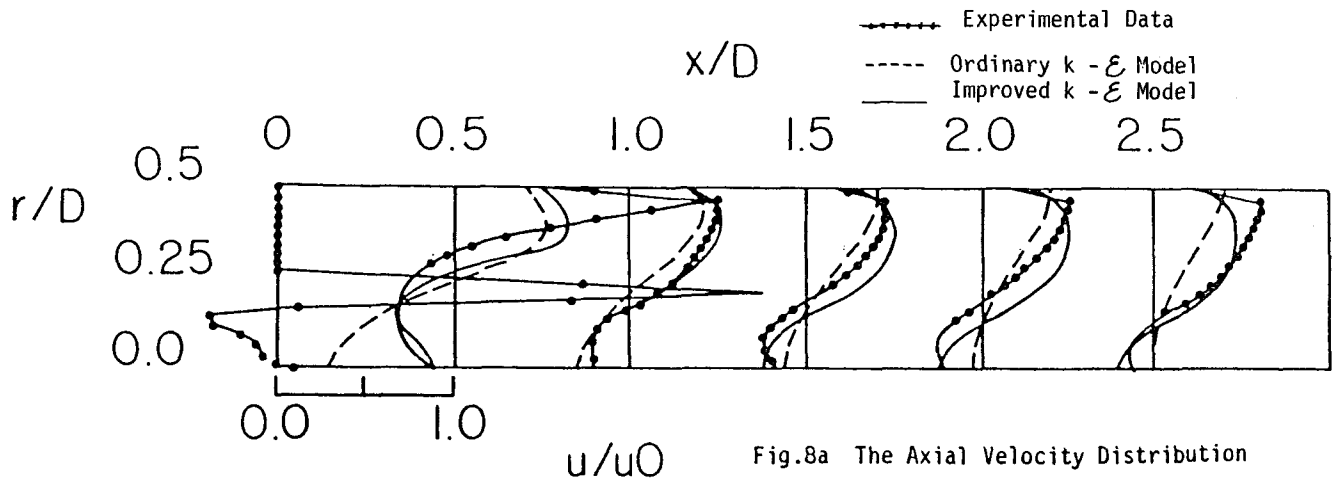


Fig.8a The Axial Velocity Distribution

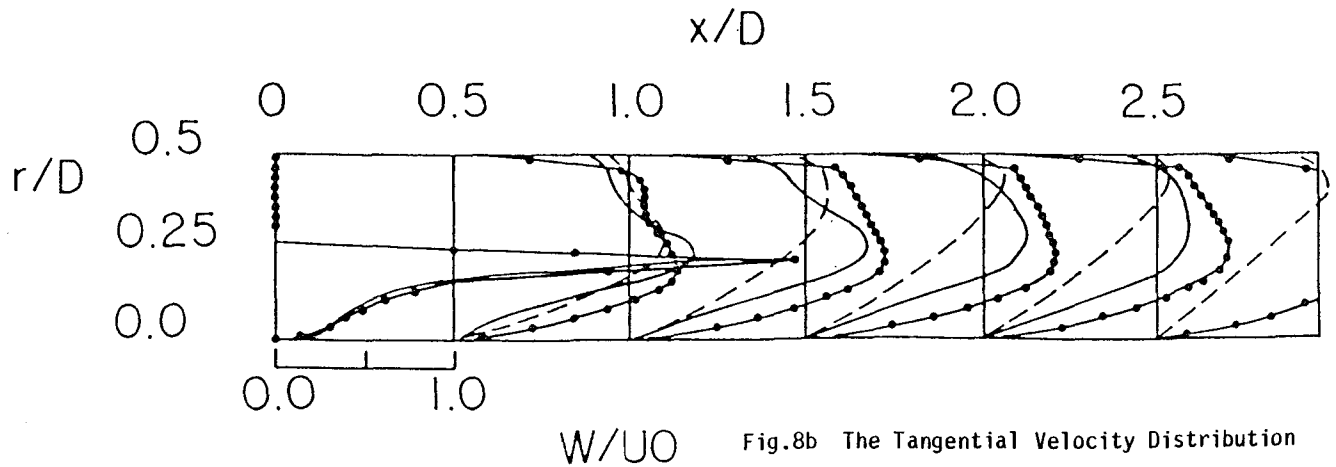


Fig.8b The Tangential Velocity Distribution

Fig.8 The Flow Field Within a Confined Sudden Expansion Swirling Flow

within the recirculating zone (Fig. 8a). These defects, however, cannot be corrected by adjusting the coefficients. The results by the new model do not show the deficiencies.

It has been found that the extra rotation term and the third-order negative dispersion term play the important roles in obtaining the correct tangential velocity profile and the proceeding vortex roll behind the recirculating zone. The stretching term makes the deficient axial velocity profile within the recirculating zone possible. The two modelings were also employed to predict the non-swirling and moderate swirling flows. Different sets of constants were required to deal with different levels of swirl for the ordinary k-ε modeling. Even under this condition, the results showed the maximum reverse flow always occurred on the axis and it never reproduced the structure of the downstream proceeding vortex roll-composite vortex structure. For the improved k-ε model all these features have been correctly and adequately reproduced.

#### DISCUSSION AND SUMMARY

With this improved modeling, computations have been carried out to study the vortex field behind a bluff body, diffusive flows, and the near wall flows. All results showed improved qualities. The success of predicting complex turbulent flows so far instills the confidence of future capabilities of dealing with complex three-dimensional turbulent flows, with accurate prediction of extra stresses, but within a reasonable amount of computing time. In this sense, it is a strong competitor for the industry-standard turbulence modeling.

It has been learned that the new coefficients  $C_0$ ,  $C_3$  need some additional adjustment. Although the physical Eq.(10) has the second order accuracy, some terms have been omitted in the modeling process for the sake of reducing the amount of computing time. Some errors must have been unavoidably introduced. For example, for the con-

vection term of the perturbation velocity,  $(\tilde{V} \cdot \nabla) \tilde{V}_\phi$ , it has three components in each momentum

equation. Only the component in the  $i$  direction has been retained. This treatment, in turn, introduced an amount of uncertainty of the coefficient  $C_3$ . Another example is in the extra rotation

term  $1/2 (\tilde{\Omega} \times \delta \tilde{r} \cdot \nabla) \nabla \phi$ .  $\delta \tilde{r}$  was considered as a local constant and was combined with  $\nabla \phi$  to form the turbulent viscosity  $\mu_T$ , which introduced a certain amount of error to the coefficient  $C_0$ .

Besides the present modeling, new modeling for the physical equation of turbulence is possible. Additional attempt for improving the capability of the non-linear modeling is worth exploring. Since the intermittent coherent structures are produced by the interactions of dissipation and dispersion, it is necessary to keep the positive dispersion term  $\nabla^2(\nabla \phi)$  in the modeling equation if the function of simulating the coherent behavior of turbulent flow is emphasized. However, for any attempt of modeling, it should be kept in mind that a compromise of accuracy and simplicity should be considered.

#### REFERENCES

1. Bo, T. and Bosman, 1989, Private Communication.
2. Cumpsty, N. A., 1989. Compressor Aerodynamics, John Wiley & Sons, Inc., NY, pp. 223-232.
3. Gao, G., 1989a, "On the Perturbation Equation of Navier-Stokes Equation," Journal of Aerospace Power, Vol. 4, No. 2, pp. 189-192.
4. Gao, G., 1989b, "A Dissipation-Dispersion Turbulence Theory and Its Modified K- $\epsilon$  Model," Journal of Aerospace Power, Vol. 4, No., pp. 97-104.
5. Hanjalic, K., 1988, "Practical Predictions by Single-Point Closure Methods, -Twenty Years of Experience," International Seminar on Near-Wall Turbulence Dubrovnik, Yugoslavia.
6. Karweit, M., "Random Incompressible Motion on Two and Three-Dimensional Lattices and into Application to the Walk on a Random Field," Frontiers in Fluid Mechanics edited by S. H. Davis and J. L. Lamley, Springer-Verlag, 1985.
7. Kline, S. J., 1981, "Universal or Zonal Modeling - The Road Ahead," Proceedings of the 1980-81 AFOSR-TTM-Stanford Conference on Complex Turbulent Flows, Vol. II, pp. 991 - 998.
8. Launda, B. E. and Spalding, D. B., 1972, "Mathematical Models of Turbulence," Academic Press, London and New York.
9. Moon, F. C., 1987, Chaotic Vibrations - An Introduction for Applied Scientists and Engineers, John Wiley & Sons, New York, pp. 205-259.
10. Orbach, R., 1986, "Dynamics of Fractal Network," Science, Vol. 231, pp. 814-819.
11. Patankar, S. V., 1981, "A Calculation Procedure for Two-dimensional Elliptic Situations," Numerical Heat Transfer, Vol. 4, No. 4, pp. 409-425.
12. Rodi, W., 1975, "A Review of Experimental Data of Uniform Density Free Turbulent Boundary fLayer," Studies in Convection. Vol. 1, Edited by B. E. Launder, Academic Press.
13. Sommeria, J., 1986, "Experimental Study of the Twoj-Dimensional Inverse Energy Cascade in a Square Box," Journal of Fluid Mechanics, Vol. 170, pp. 139-168.
14. Taubee, D. B., 1987, "The Round Jet Experiment and Inferences on Turbulence Modeling," 6th Symposium K- $\epsilon$  Model," Journal of Aerospace Power, Vol. 4, No. 1, pp. 97-104.
15. Xu, H. and Gao, G., 1990, "Computation of Confined Turbulent Swirling Flow With Sudden Expansion," submitted to the Conference of Turbulence Modeling, Yugoslavia, September 1990.